Comparison of data from co-located sensor packages and implications for dispersion modeling: An *in situ* case study of rugged versus low-threshold anemometers and natural- versus forced-ventilation solar shields

Frank J. Gouveia and Ron L. Baskett

Health & Ecological Assessment Division
Lawrence Livermore National Laboratory
Livermore, California

Abstract

We compared 27 days of 15-minute-average data from two sets of co-located wind and temperature sensors at 10- and 40-m levels on a tower at Lawrence Livermore National Laboratory,. One anemometer set was rugged and the other was more sensitive with a lower threshold. At moderate winds ($2<U<10$ m/s) wind speed and direction between the two sets of sensors were strongly correlated. At low winds ($U<2$ m/s), the two sets produced small discrepancies due to different thresholds and calibration methods for the wind speed sensors. Stability class (Modified Sigma Theta method) was found to be the same for each sensor package for 76% of the study period and within one stability class for 94% of the time. We also compared temperature data from the naturally aspirated solar shields with data from fan-aspirated shields. The tendencies were expected and quantified, large temperature differences when the wind speed was low and insolation was great. Temperature difference was greater than 1°C about 15% of the study period and greater than 0.5°C about 39% of the time.

Introduction

Since the early 1980s, Lawrence Livermore National Laboratory (LLNL) in Livermore, California has collected on-site meteorological data for use in regulatory-driven dispersion modeling and for emergency preparedness and response. Data from the dual-purpose tower has been collected on a workstation using software developed by the DOE Atmospheric Release Advisory Capability (ARAC) at LLNL. Consequently, the original sensors on the tower conformed to the ARAC network design which included rugged wind sensors that only needed annual calibration and maintenance. The reliable Handar 540 data logger and durable sensors met these criteria although the meteorological sensors did not meet all PSD (Prevention of Significant Deterioration) guidelines (EPA 1980) and further guidance later developed by DOE (1991). In response to recent Bay Area Air Quality Management District and DOE (1991) recommendations to monitor meteorological conditions with greater sensitivity, we installed a new set of sensors during October of 1995. We took advantage of this opportunity to acquire a simultaneous database from both sets of sensors.

Previous field comparisons of meteorological sensors (Finkelstein 1986, Tanner 1996) have shown that wind tunnel experiments may not reveal the true character of a wind vane's response

to natural wind and turbulence conditions. We designed our study to compare the data from the two juxtaposed sets of sensors and attempt to explain differences in the measurements. In addition we explore the effect of these differences on dispersion calculations by comparing Pasquill stability class computed using the Modified Sigma Theta method. We also use the datasets to compute the mean composite downwind concentration profile in a Gaussian dispersion model.

Description of field experiment

Descriptions of the site and tower

LLNL is located on the eastern side of the Livermore Valley, about 30 miles east of Oakland, California. The meteorological tower is located near the northwest corner of LLNL site with an elevation of 174 m. The surface topography slopes up gently towards the southeast with a grade of approximately 12 m vertically in 1 km.

The 40-m LLNL meteorological tower is located where it is exposed to relatively open fetches for over 150 m in all directions. The vegetation surrounding the tower consists mostly of annual grasses. The surface roughness is about 0.15 m and the zero-plane displacement is 0.5 cm (Chapman & Gouveia, 1988). The largest nearby feature is a north by south line of eucalyptus trees about 150 m to the east. A housing development is about 250 m to the west, commercial buildings are located 300 m to the north. The closest substantial structure towards the south is approximately 500 m away from the tower.

The sensors are fixed to crossarms that are on 2-m long booms extending off the west side of the tower at 10 and 40 m above the ground. The booms are raised and lowered by means of a manual-crank elevator. For this study, both the Handar and Met One sensor wind sets were mounted on the booms. The Handar crossarm was oriented north/south with the wind vane on the north end. The Met One crossarm was attached to the Handar crossarm with the wind vane on the west end.

Variables measured by both systems at both levels included horizontal wind speed and direction, standard deviation of wind direction (σ_θ), and temperature. Additionally, the Met One system included a temperature at 2 m and a solar radiation sensor.

Maintenance is performed according to EPA guidance (EPA 1987 and 1990). However, delays in installing the Met One system forced us to postpone the regular calibration of the Handar sensors. This deferred maintenance may have influenced the response of the Handar 431A vane and 430A cups. Torque measurements on the wind sensors are pending as well as the calibration of the thermistors.

Data acquisition

The Handar and Met One systems were connected to separate but identical Handar 540 data loggers running similar acquisition programs synchronized to the same clock. The instruments were polled every second and 15-minute averages were stored on each 540 logger. The data were periodically transferred via modem to a Sun workstation. σ_θ was calculated by both systems by the same algorithm following Yamartino (1984).

Sensors

Physical description

The following specifications of the Handar and Met One sensors have been taken from the respective manufacturer's literature. Table 1 summarizes the sensors used in this study.

Anemometry

Both the Handar 431A and Met One 020C wind direction sensors are vanes using precision potentiometers. The head or counter balance of the Handar vane has a larger surface area than the Met One vane.

The Handar 430A and Met One 010C wind speed sensors are 3-cup design. The 430A uses a rotating magnetic field in proximity to a Hall Effect device to produce a pulse output directly proportional to wind speed. The 010C uses a slotted chopper disk to produce a pulsed output that is converted to a voltage proportional to wind speed. The starting threshold, distance constant and damping ratio for all wind sensors is presented in Table 2. The damping ratio, ξ, for the Handar 431A vane was computed with the formulation from Wang (1979),

$$\xi = \sqrt{r / (2 \cdot D)}, \tag{1}$$

where r is the vane arm length and D is the distance constant.

The Handar 431A vane meets PSD guidelines (EPA 1980) for starting threshold (≤ 0.5 m/s) and distance constant (≤ 5 m) but is just outside the PSD range for damping ratio (0.4 - 0.6). The Met One 020C vane meets all PSD guidelines.

Temperature

The Handar and Met One systems both utilize the YSI 44006 single-bead thermistor. The standard lookup tables located in the Handar 540 firmware converted thermistor resistance to temperature units. This thermistor shows an absolute accuracy of ± 0.5 °C of a standard.

Solar shields

The solar shield for the two Handar thermistors is the model 442A Convection-Aspirated Shield. This shield takes advantage of the natural flow of air for ventilation.

The Met One system includes the 076B Radiation Shield. This shield includes a motor with a fan that provides a constant flow of air past the temperature and humidity sensors. This shield uses an AC fan to produce a flow of 2.5 m/s in the inner sample tube and 5 m/s in the air space between the nested tubes.

Table 1 – Sensor types and model numbers used in this study.

Variable	Type	Handar	Met One
Wind direction	Vane	431A	020C
Wind speed	3-cup	430A	010C
Air temperature	Thermistor	YSI 44006	YSI 44006
Solar shield	Natural	442A	---
Solar shield	Forced	---	076B
Insolation	Licor	---	096-1

Table 2 – Specifications of the anemometers and vanes.

Model	Starting threshold	Distance constant	Damping ratio
431A vane	0.5 m/s	5.0 m	0.2*
430A cups	0.5	5.0	---
020C vane	0.3	<1.0	>0.4*
010C cups	0.3	<1.6	---

* Values computed from Eq. 1.

Radiometer

Incoming solar radiation is measured by the Licor-type Met One model 096-1 Solar Radiation Sensor. The radiometer is electronically connected to the Met One system.

Study period

Mutual data collection started on 11 October 1995 and continued to 30 November 1995. An interruption in the data collection created a gap in the comparison data during the first two weeks of November. This interruption resulted in two comparison periods, the first with 1512 fifteen-minute records and the second with 1090 records. Preliminary analysis of both periods indicated no significant differences in the data sets. Therefore, all subsequent analysis combined data from both periods.

The wind rose for the study period (Figure 1) shows that 10 of the 16 compass directions have a frequency over 5%. The data for this wind rose was taken from the 10-m level of the Met One system. The weather during the study period was typical for autumn at LLNL. The average annual wind speed at the site is 2.3 m/s (Gouveia and Chapman 1989). The fall study period reflects a relatively calm period of the year. The average wind speed for the study period as measured by the Met One sensors was 1.8 m/s at the 10-m level. The average wind speed in the predominate wind directions was somewhat higher than the all-direction average. For winds from the NE the average was 2.5 m/s at the 10-m level, from the SW the average was 2.3 m/s. There was no measurable precipitation although fog was observed several times in the morning hours.

Comparisons between sensor data sets

Wind direction

We compare wind direction data when the wind speed was greater than 2 m/s. A separate analysis of low wind speed cases is discussed in a following section. Figures 2 and 3 show the highly correlated wind direction data as measured by the two sensors at 10 and 40 m. Figures 4 and 5 plot the difference between the wind vanes against the Met One vane position. This same wavy pattern was described in Lockhart (1989). There seems to be a consistent 3° deviation between the Met One and the Handar vanes at the 10-m level which is due to alignment difference. Some bias may be due to non-linearity of the potentiometers, out-of-round, or signal conditioning errors although these errors are typically not greater than ±3° (EPA 1990). Most of the wind vane difference data is within this range.

Wind Speed

The wind speed as measured by the two systems shows a very good correlation as shown in figures 6 and 7, especially at speeds greater than 2 m/s. The small difference at the low winds may be due to different manufacturer's recommended conversion from shaft rotation to m/s. Average wind speed measured at 10 m was 1.8 m/s for the Met One system and 1.5 m/s for the Handar system. At the 40-m level the average wind speed for the Met One and Handar systems was 2.5 and 2.1 m/s, respectively.

Sigma Theta

The largest difference between measured quantities is found in the σ_θ data. Figures 8 and 9 show σ_θ as measured by the Met One versus σ_θ from the HANDAR system for the 10 and 40 m levels. The low winds (< 2 m/s) were excluded in these figures due the large differences of σ_θ in this range. That the Handar σ_θ was sometimes larger than the Met One value can be explained by the Handar's smaller damping ratio. EPA (1990) states that vanes with smaller damping ratio, such as the 431A, will report more variability from the same turbulent flow than a vane with a

larger damping ratio. Table 3 displays the percent occurrence of selected ranges of the difference in σ_θ readings. Note the consistent values between the two levels in this table when the wind speed is limited.

Temperature

Ambient air temperature as measured by both systems follows a predictable pattern as described in Tanner (1996). Figure 10 shows the comparison between the temperature measurements at 10 m. The 40-m temperature shows the same pattern as the 10-m data although for a slightly narrower range of temperature. Readily apparent in this plot is the tilt of the data points for the natural ventilated solar shield towards higher daytime temperatures and lower nighttime temperatures. Figure 11 shows the temperature difference between the systems plotted with wind speed for the 10-m level (again, the 40-m graph was omitted for redundancy). Figure 12 shows the same temperature difference plotted against solar radiation. The largest values of temperature difference occur when strong insolation corresponds with weak winds.

An attempt was made to create a simple adjustment to the temperature data from the naturally ventilated shield. A function was made based on linear regression,

$$\Delta T = 0.143 * U - 0.00386 * R, \quad (2)$$

where U is the wind speed in m/s and R is incoming solar radiation in w/m^2. The constant term was close to zero and ignored. The coefficients reveal that, for our site and this data set, solar radiation causes more temperature error than the wind speed due to the unventilated shields. After applying the above adjustment to the Handar temperature data the standard error between the Met One and Handar systems was reduced from about 0.9 to 0.6°C. Figure 13 shows the adjusted naturally aspirated temperature and the fan-aspirated temperature data. More improvement could be achieved with knowledge of the solar radiation incident on the sides of the naturally aspirated shields.

Computed variables

Stability by MST

Stability, as classified by Pasquill stability categories, was computed using the Modified σ_θ method (a.k.a. lateral turbulence and wind speed method) described in EPA (1987). This method uses σ_θ for an initial estimate of Pasquill class which is adjusted with wind speed and time of day. The computation is made separately for every 15-minute averaging period, each level (10 and 40 m), and each system. No attempt was made to smooth the stability class with time. Tables 4 and 5 show the percent occurrence of Pasquill category for the two systems for the 10- and 40-m

Table 3 – Percent occurrence of the difference of σ_θ between the Handar and Met One systems for the 10- and 40-m levels.

Range of difference between σ_θ values	All wind speeds		$WS_{10} \geq 2$ m/s	
	10 m	40 m	10 m	40 m
± 25	90	99	--	--
± 20	87	98	--	--
± 15	83	96	99	99
± 10	78	93	97	97
± 5.0	66	82	89	89
± 2.5	54	69	81	81
± 1.0	38	50	69	66

levels, respectively. These analysis show that the Pasquill category is almost always the same between the systems. In fact, as Table 6 shows, each system produces the same stability category 75 to 80% of the time. The systems are within one class about 95% of the time.

Period of low winds

A 16-hour period of winds less than 2 m/s beginning in the evening of 19 October was identified for additional study. Figure 14 shows time series of wind speed for each system and the difference of wind direction between the two systems. The approximately 0.3 m/s separation in the wind speed traces are a result of different methods converting cup rotation to speed as described above. At about 1 A.M. and continuing for almost 5 hours, the 430A anemometer reported 0.0 m/s while the lower threshold 010C detected small pulses as much as 0.6 m/s for a few 15-minute periods. Figure 15 shows a time series of the wind direction from both the low-threshold and rugged wind vanes. The vanes track very well when the wind was between from 0.5 and 2.0 m/s, but then deviate when the winds fall below 0.5 m/s (as measured by the 010C).

Table 4 – Distribution of the 2587 realizations of P-G stability class as computed for the Handar and Met One systems at the 10-m level. Values are presented in percent.

	Handar						
Met One	A	B	C	D	E	F	All
A	8.7	1.0	0.2	0.1	-	-	10.1
B	0.5	5.9	0.5	-	-	-	6.9
C	-	1.1	8.2	0.5	-	-	9.9
D	-	-	0.5	16.5	2.5	2.4	21.9
E	-	-	-	2.7	8.4	3.4	14.5
F	-	-	-	3.1	5.5	28.2	36.8
All	9.3	7.9	9.4	22.9	16.4	34.0	

Table 5 – Same as Table 4 but for the 40-m level.

	Handar						
Met One	A	B	C	D	E	F	All
A	9.6	0.3	-	-	-	-	9.9
B	1.0	5.5	0.3	-	-	-	6.8
C	0.2	1.5	9.4	0.3	-	-	11.5
D	-	-	0.6	21.0	4.4	2.1	28.1
E	-	-	-	3.0	8.3	3.7	15.1
F	-	-	-	0.4	1.7	26.6	28.7
All	10.9	7.3	10.2	24.7	14.5	32.4	

Table 6 – Percent difference in stability class (Met One minus Handar) for both levels (A=1 ... F=6).

Difference in Class	10 m	40 m
-2	3	2
-1	8	9
0	76	80
1	10	8
2	3	1

Wind rose statistics

Wind roses were made for the 10-m level and are presented as Figures 1 and 16, for the Met One and Handar systems, respectively. The 40-m data show the same patterns and were not included here for brevity. Wind rose statistics are summarized in Tables 7 and 8 and described below.

Table 7 is a histogram of wind direction for all wind vanes. Wind speeds less than 0.5 m/s are considered below threshold for both systems and wind direction measurement is unreliable. At these low winds the actual wind direction is ignored and the wind is distributed evenly among all wind directions. The difference in frequency between systems at the same level is never greater than three percent.

Frequency distribution of wind speed for all anemometers are presented in Table 8. It is again evident in this table that the 010C wind speed sensors report larger values than the 430A sensors. This result is the most compelling reason for switching to the low-threshold anemometer and vane. Past annual wind roses for LLNL (Gouveia and Chapman 1989, and Harrach, et al. 1994) feature a frequency of winds less than 0.5 m/s of about 14% using the Handar sensors. It is expected that, with the lower threshold instruments, the frequency of winds in this lowest class will be less than 5% in the annual wind rose.

Table 7 – Percent of wind direction for both systems at both levels. Wind speeds less than 0.5 m/s are distributed evenly among all wind directions.

Direction	10 m		40 m	
from	Met One	Handar	Met One	Handar
NNE	9.1	10.0	7.9	8.8
NE	11.1	12.0	13.0	13.0
ENE	5.1	4.9	5.5	4.5
E	5.3	3.7	5.2	5.9
ESE	7.5	5.0	5.2	4.7
SE	4.7	3.9	3.9	3.5
SSE	4.3	3.5	3.1	3.1
S	11.1	8.6	9.5	8.5
SSW	8.9	8.9	8.8	8.4
SW	8.5	9.8	11.2	12.0
WSW	9.0	9.3	9.4	10.0
W	5.9	7.9	7.0	7.2
WNW	2.7	3.3	2.5	2.6
NW	2.3	3.2	2.8	2.4
NNW	2.3	3.0	3.2	3.0
N	2.3	2.9	1.9	2.5

Table 8 – Percent of wind speed ranges for both systems and both levels.

		Wind Speed class (m/s)				
System	Level	0.0-0.4	0.5-2.9	3.0-4.9	5.0-6.9	≥7.0
Met One	10 m	8.9	54.7	27.8	7.7	0.9
Handar	10 m	31.7	37.6	23.4	6.4	0.8
Met One	40 m	1.4	45.8	33.2	15.5	4.0
Handar	40 m	13.4	42.4	30.7	10.8	2.8

Dispersion model

The regulatory model, CAP88-PC (EPA 1992), was run to investigate the implication of using meteorological data from the two systems. CAP88-PC is an EPA-approved air-dispersion and dose-assessment model. The current study just looks at the air dispersion capability of CAP88-PC. The model estimates downwind concentrations with a Gaussian dispersion algorithm. The meteorological data must be processed into joint-frequency tables of wind direction and stability class as well as tables of average and harmonic average wind speed. The model estimates the concentrations at receptors arranged in polar coordinates with 16 radials and 19 distance rings from 100 to 1000 m. This scheme yielded a total of 304 individual receptors. The concentration at a given receptor is affected by the frequency of wind in that direction as well as the frequency of stability class and the average wind speed.

A fictious but plausible source was entered into the model. The source was a 30-m high stack with exit velocity of about 8.0 m/s and diameter of 1.2 m. The effluent was gaseous, neutrally buoyant and had no settling. A unit source strength was used to produce relative concentrations. All parameters for both runs were the same except for the source of the meteorological data. Figure 17 compares the average relative concentration of the two model runs as a function of downwind distance between 0.1 and 1.0 km. The average relative air concentration is an average of the relative concentrations from all 16 directions at a particular distance from the source. The relative concentrations are 10-20% lower for the CAP88-PC run using the Met One meteorological data. This may be due in part to the higher wind speeds of this data set. The higher winds increase the dilution of the plume and allow for less plume rise of the momentum-driven effluent. The higher winds tend to move the stability class towards neutral, but this may be partially offset by smaller values of σ_θ from the Met One vane. The relative concentrations for 185 of the 304 receptors (about 60%) was lower for the model run using Met One data.

Conclusions

- Housing thermistors in fan-aspirated shields significantly improves the accuracy of temperature measurements over the naturally aspirated shields. More analysis is necessary to determine if temperature measurements made with thermistors in fan-aspirated shields is adequate for $\Delta T/\Delta z$ estimation.

- Improvement in the accuracy of air temperature measurements made in naturally aspirated solar shields can be achieved by compensating for wind and solar radiation.

- The rugged, higher threshold wind sensors may be appropriate for meteorological monitoring in windy or hostile environments.

- More sensitive wind sensors produce two differences:

⇒ More information about wind at very low wind speeds.

⇒ Smaller σ_θ due to higher damping.

- Estimates of dispersion will be affected by slightly higher wind speeds measured by the Met One wind sensors. The slightly higher wind speeds will decrease downwind air concentrations due to increased dilution of the plume.

Acknowledgments

The authors would like to thank the following individuals who were instrumental in the completion of this work. Gary Bear and Jon Welch must be recognized for their expert technical support when installing the new monitoring system. Brent Bowen's efforts are appreciated for his assistance with the interpretation of the results. Valuable and timely help came from Clyde Davis at Handar and Dennis Recla and Ron Ralston at Met One. Work performed under the auspices of the U.S. Department of Energy at Lawrence Livermore National Laboratory under contract W-7405-Eng-48.

References

Chapman, K.R. and F.J. Gouveia, 1988: Wind Flow Study: July 1987 and November-December 1987, UCID-21360, Lawrence Livermore National Laboratory, Livermore, CA.

DOE, 1991: Environmental Regulatory Guide for Radiological Effluent Monitoring and Environmental Surveillance, DOE/EH-0173T, U.S. Department of Energy, Assistant Secretary for Environment, Safety and Health, Washington, D.C..

EPA, 1980: Ambient Monitoring Guidelines for Prevention of Significant Deterioration (PSD), EPA-450/4-80-012, U.S. Environmental Protection Agency, Office of Air Quality, Research Triangle Park, NC.

EPA, 1987: On-Site Meteorological Program Guidance for Regulatory Modeling Applications, EPA-450/4-87-013, U.S. Environmental Protection Agency, Office of Air Quality, Research Triangle Park, NC.

EPA, 1990: Quality Assurance Handbook for Air Pollution Measurement Systems, Volume IV --- Meteorological Measurements, EPA-600/4-90-003, U.S. Environmental Protection Agency, Office of Research and Development, Research Triangle Park, NC.

EPA, 1992: User's guide for CAP88-PC, Version 1, 402-B-92-001, U.S. Environmental Protection Agency, Office of Radiation Programs, Las Vegas, NV.

Finkelstein, P.L., J.C. Kaimal, J.E. Gaynor, M.E. Graves, and T.J. Lockhart, 1986: Comparison of wind monitoring systems: Part I: In situ sensors, *J. of Atmos. and Oceanic Technol.*, **3**, 583-593.

Gouveia, F.J. and K.R. Chapman, 1989: Climatology of Lawrence Livermore National Laboratory, UCID-21686, Lawrence Livermore National Laboratory, Livermore, CA.

Harrach, R.J., et al., 1994: Environmental Report 1994, UCRL-50027-94, Lawrence Livermore National Laboratory, Livermore, CA.

Lockhart, T.J., 1989: Accuracy of the Collocated Transfer Standard Method for Wind Instrument Auditing, *J. of Atmos. and Oceanic Technol.*, **6**, 715-723.

Tanner, B.D., E. Swiatek, and C. Maughan, 1996: Field comparisons of naturally ventilated and aspirated radiation shields for weather station air temperature measurements, Proceedings from the 22nd Conf. on Agricultural & Forest Meteorology with Symposium on Fire & Forest Meteorology, American Meteorological Society, Boston, Mass..

Wang, J.Y., and C.M.M. Felton, 1979: Instruments for Physical Environmental Measurements, Milieu Information Service, Inc.

Yamartino, R.J., 1984: A comparison of several "Single-pass" Estimators of the Standard Deviation of Wind Direction, *J. Climate and Applied Meteorology*, **23**, 1362-1366.

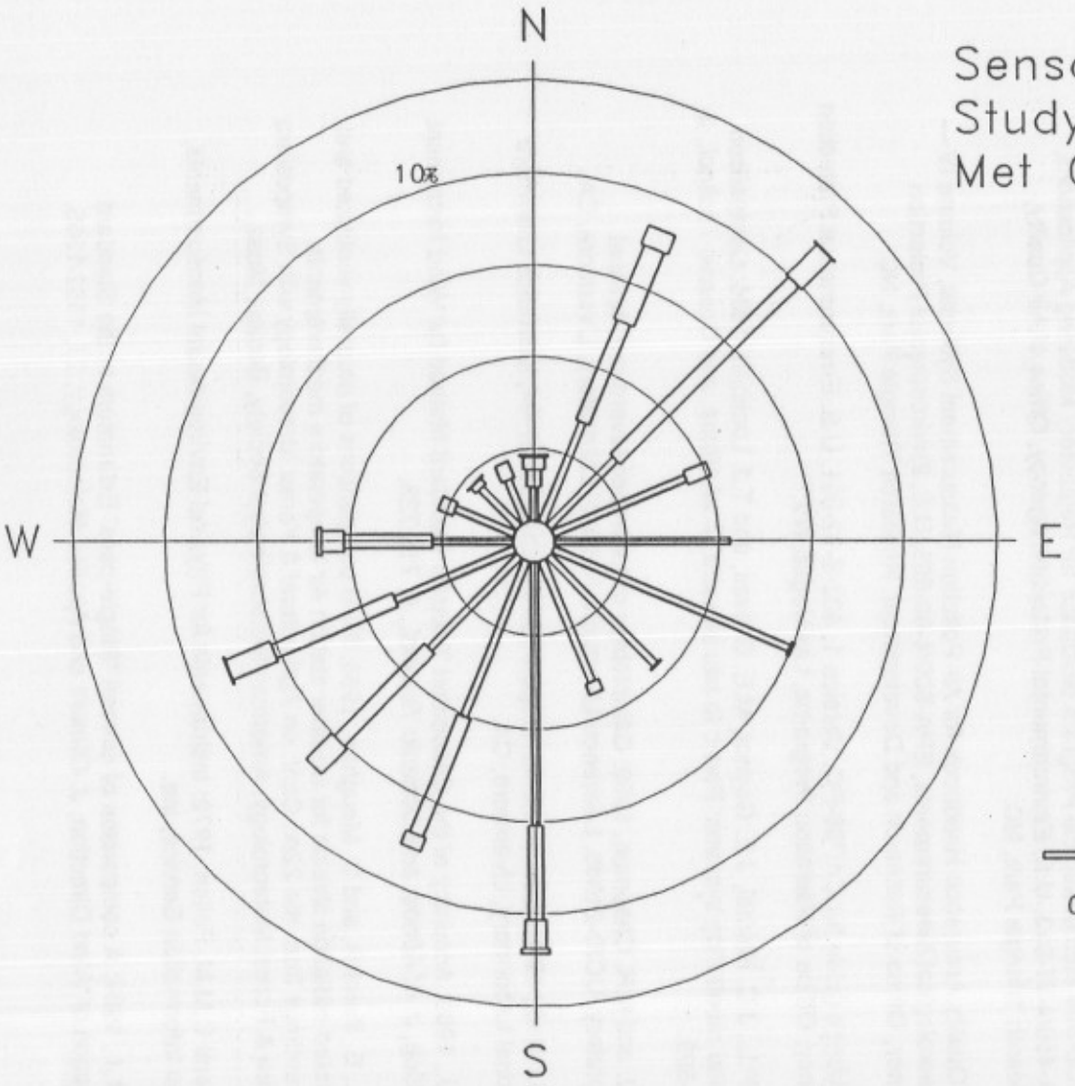

Sensor Comparison at LLNL
Study Period: Oct & Nov 1995
Met One System -- 10 m

Wind Speed (m/s)

0.5-2 2-4 4-6 >=6

Calms: 8.9%

Figure 1. Wind rose for the study period. Wind data was taken from the Met One system at the 10-m level. Figure 16 is a similar wind rose for the Handar system.

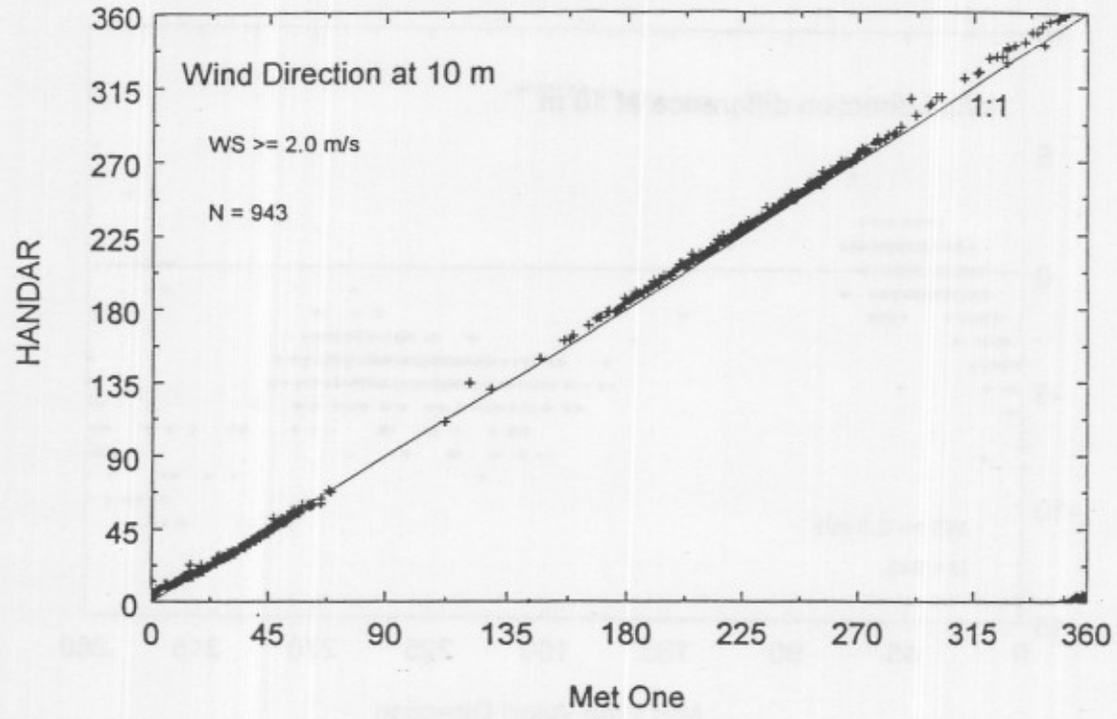

Figure 2. Comparison of wind direction readings for wind speeds 2.0 m/s or greater from the 10-m level.

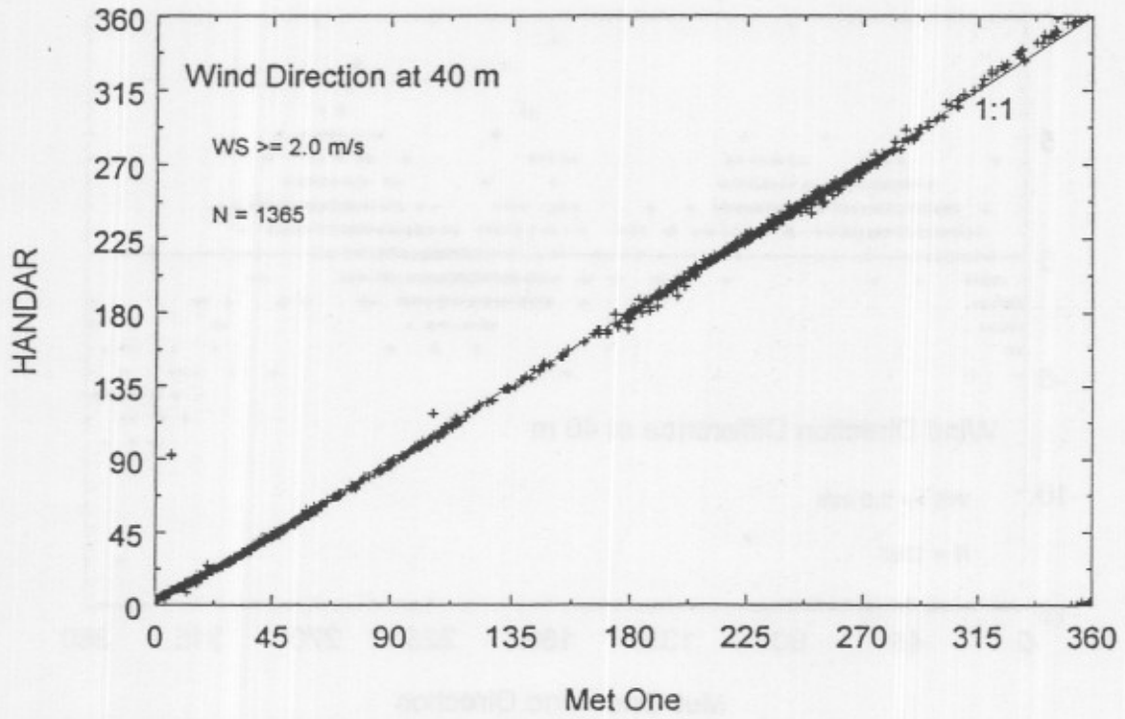

Figure 3. Same as Figure but for the 40-m level.

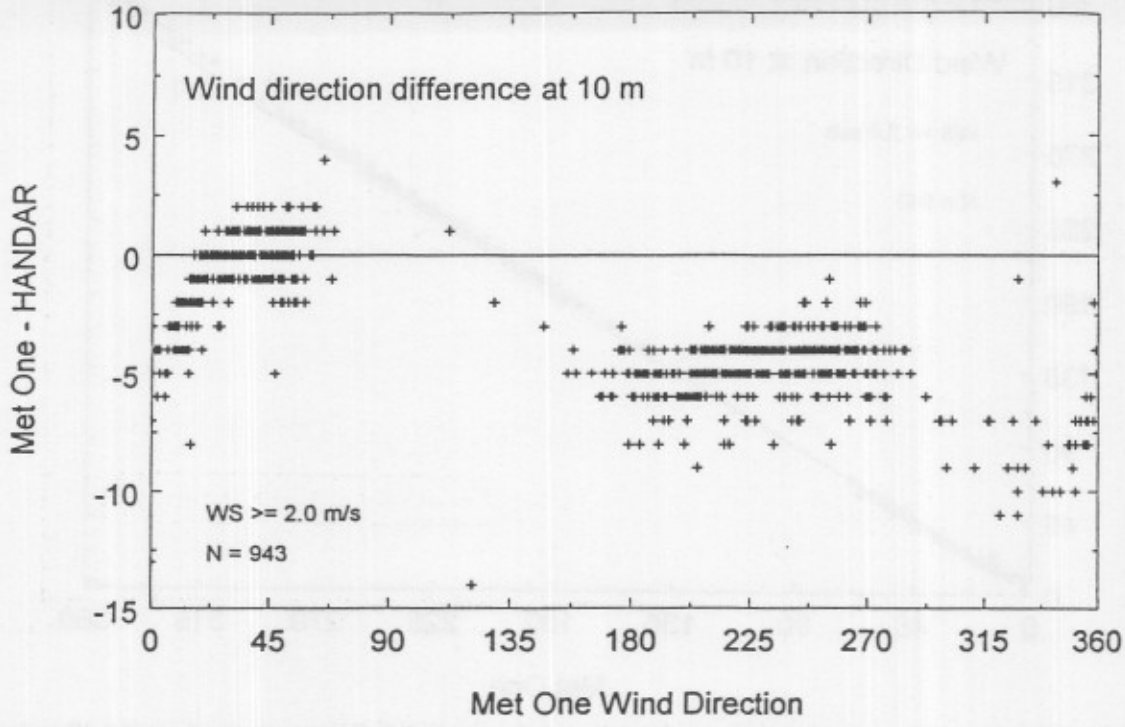

Figure 4. Difference in wind direction readings plotted against the wind direction from the Met One for wind speeds 2.0 m/s or greater at the 10-m level.

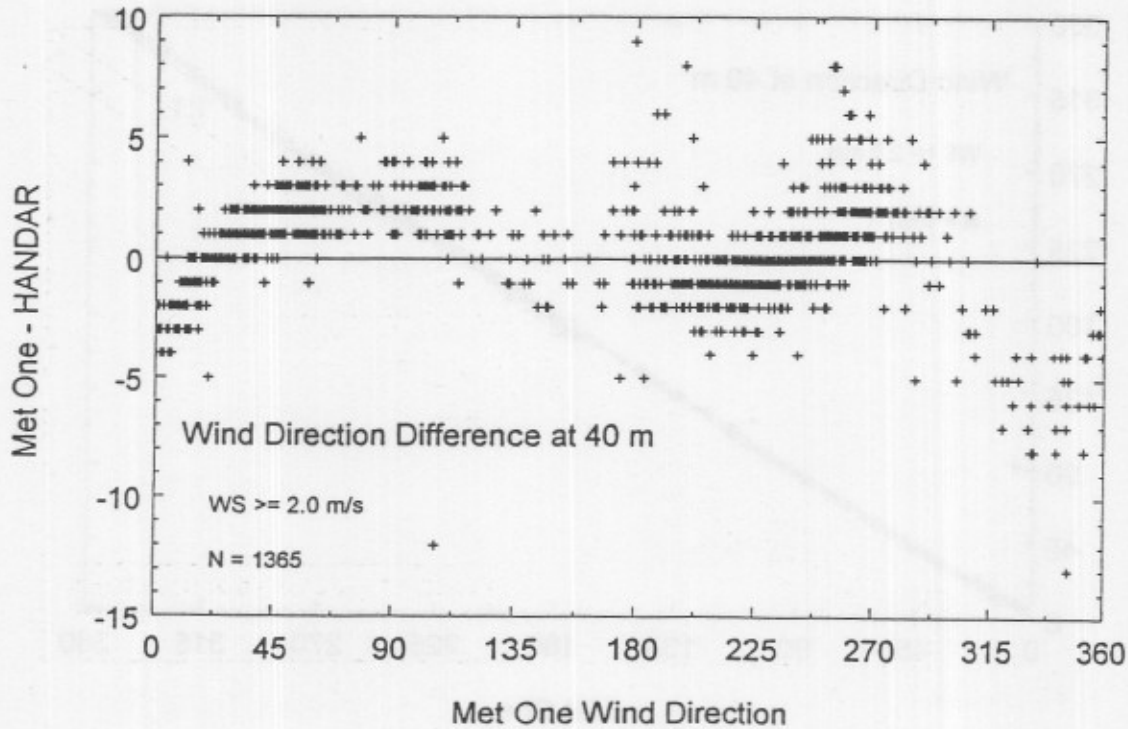

Figure 5. Same as Figure 4 but for the 40-m level.

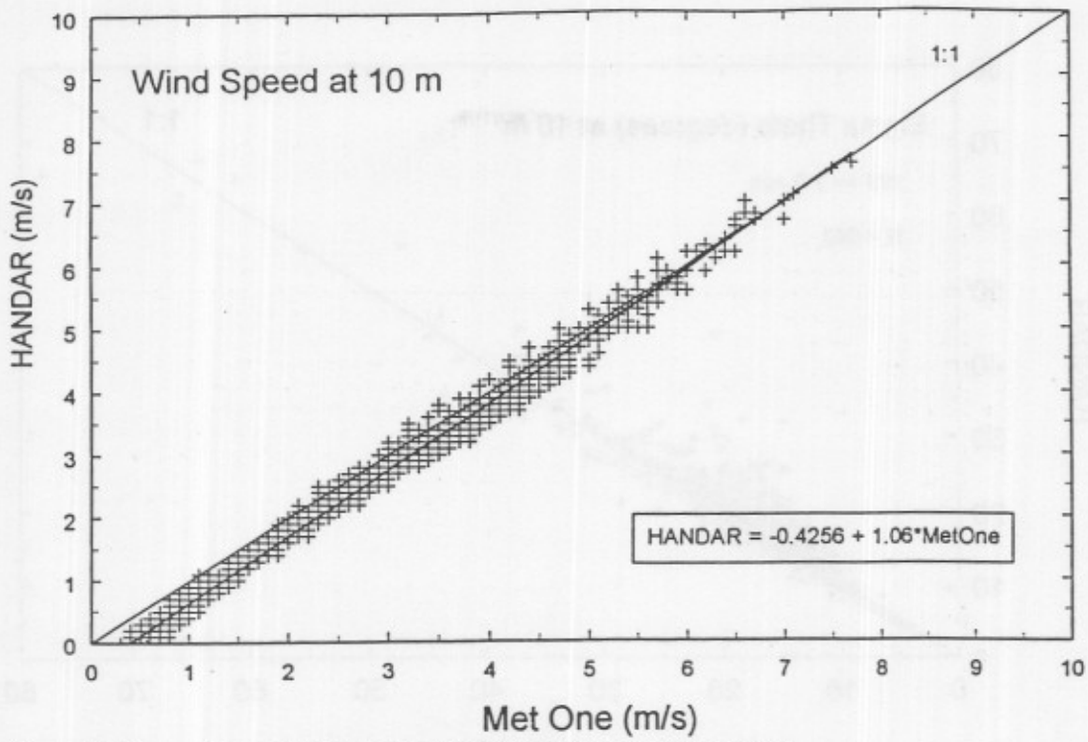

Figure 6. Comparison of wind speed readings from the 10-m level.

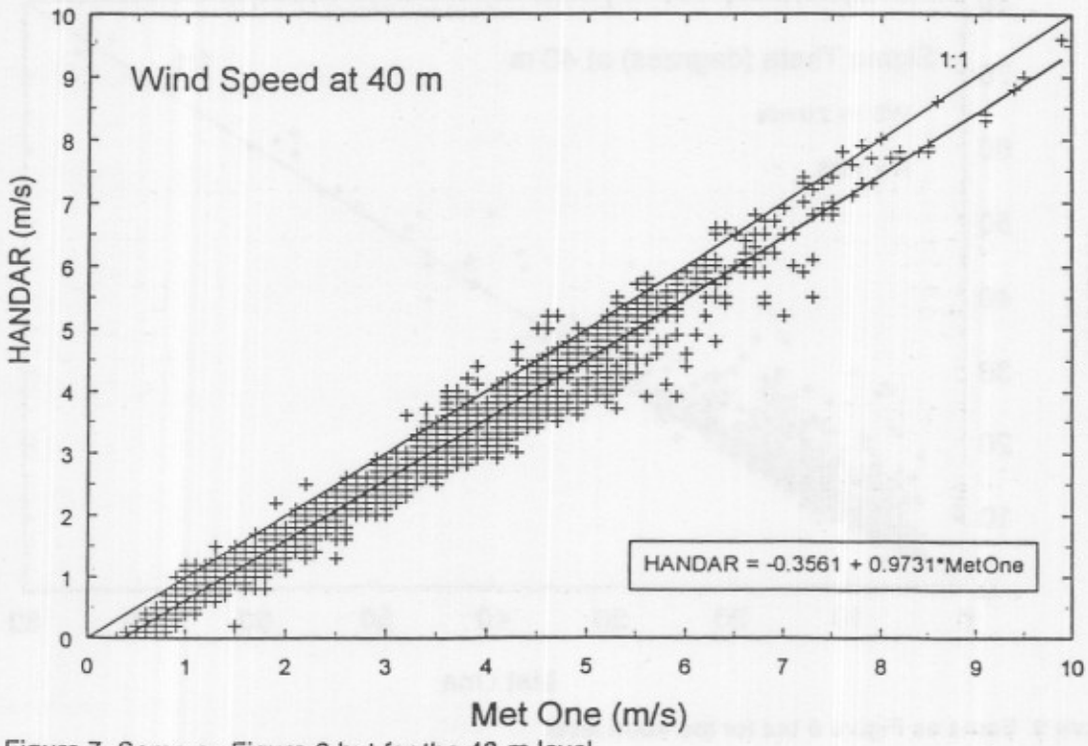

Figure 7. Same as Figure 6 but for the 40-m level.

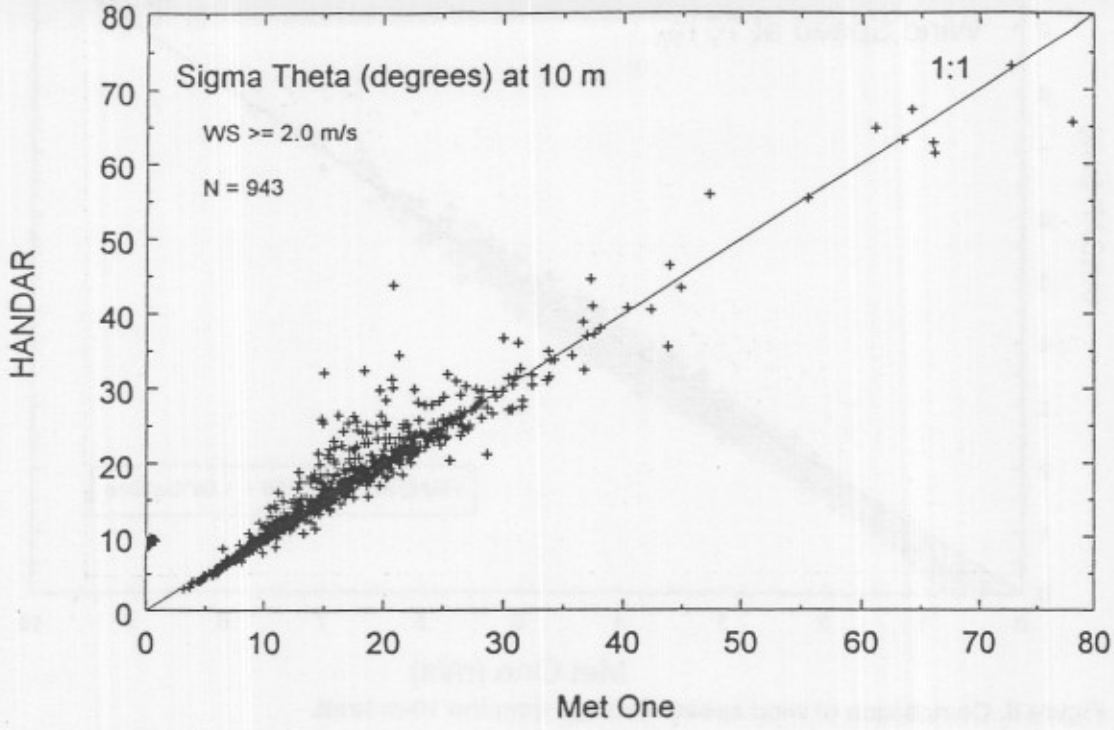

Figure 8. Comparison of σ_θ from the 10-m level.

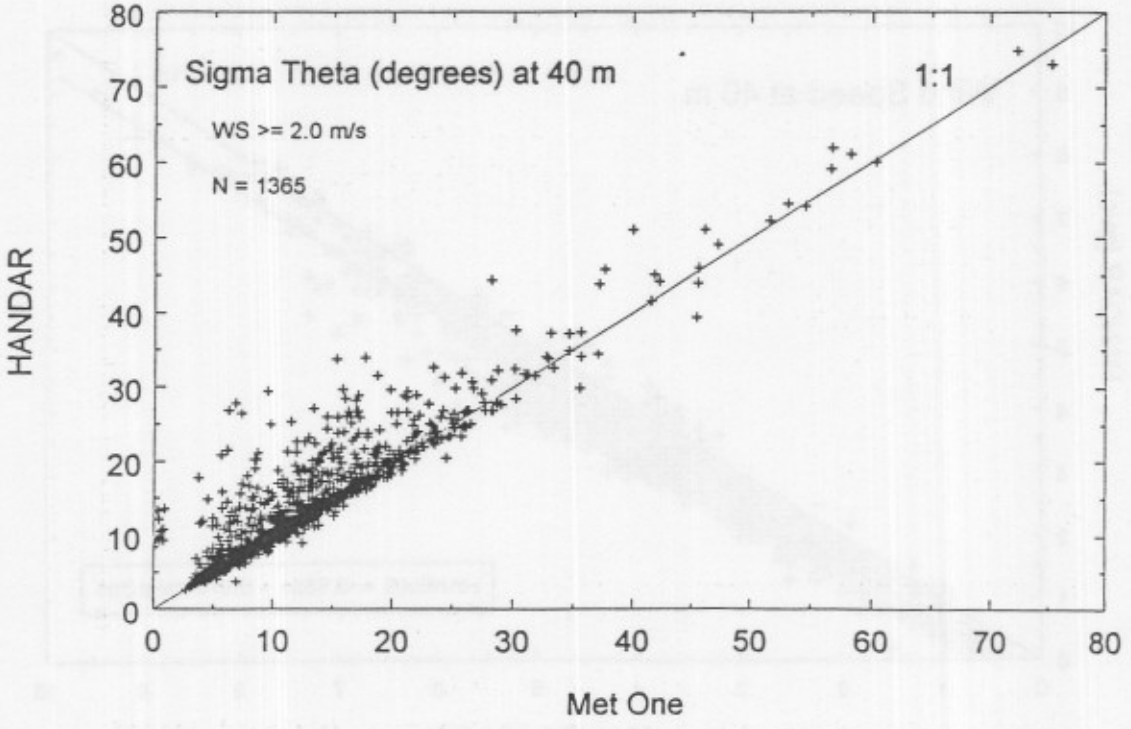

Figure 9. Same as Figure 8 but for the 40-m level.

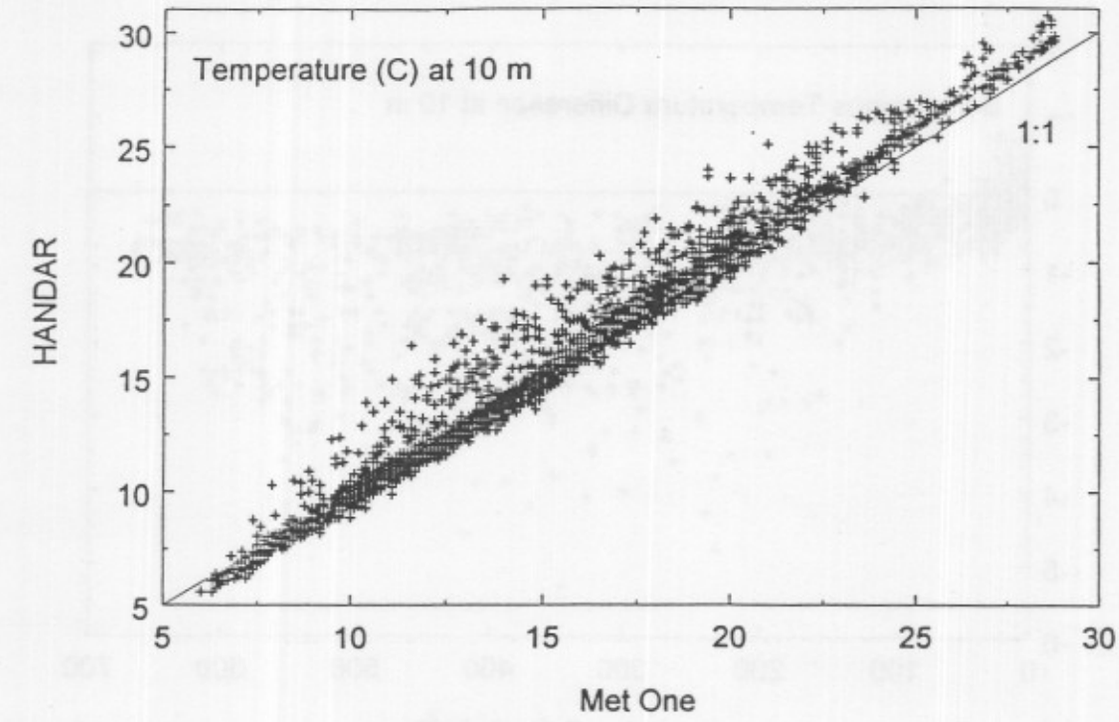

Figure 10. Comparison of temperature from the 10-m level.

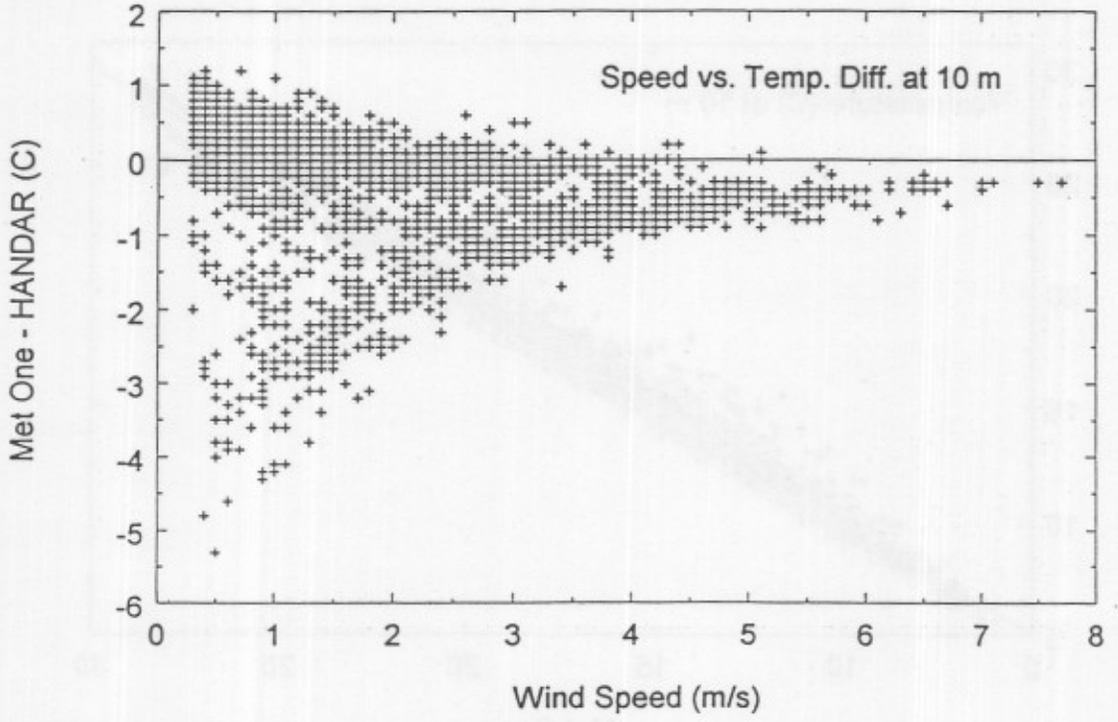

Figure 11. Difference in temperature from the 10-m level plotted against Met One wind speed.

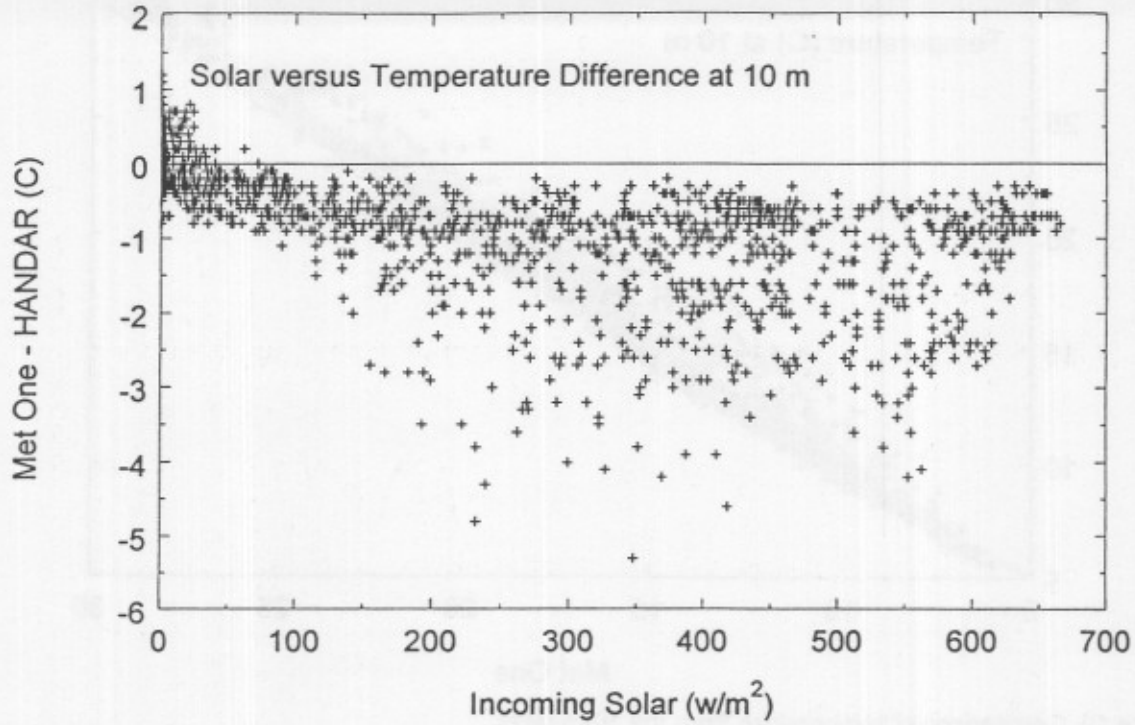

Figure 12. Difference in temperature from the 10-m level against incoming solar radiation.

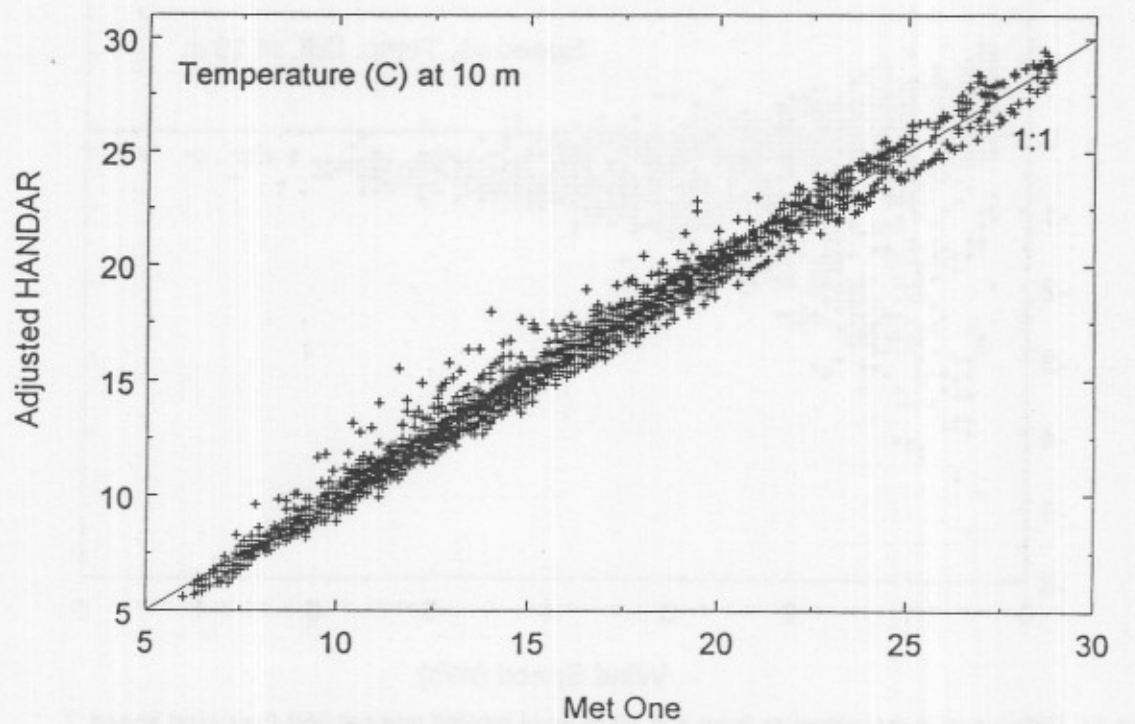

Figure 13. Met One temperature versus Handar temperature adjusted for wind speed and solar radiation.

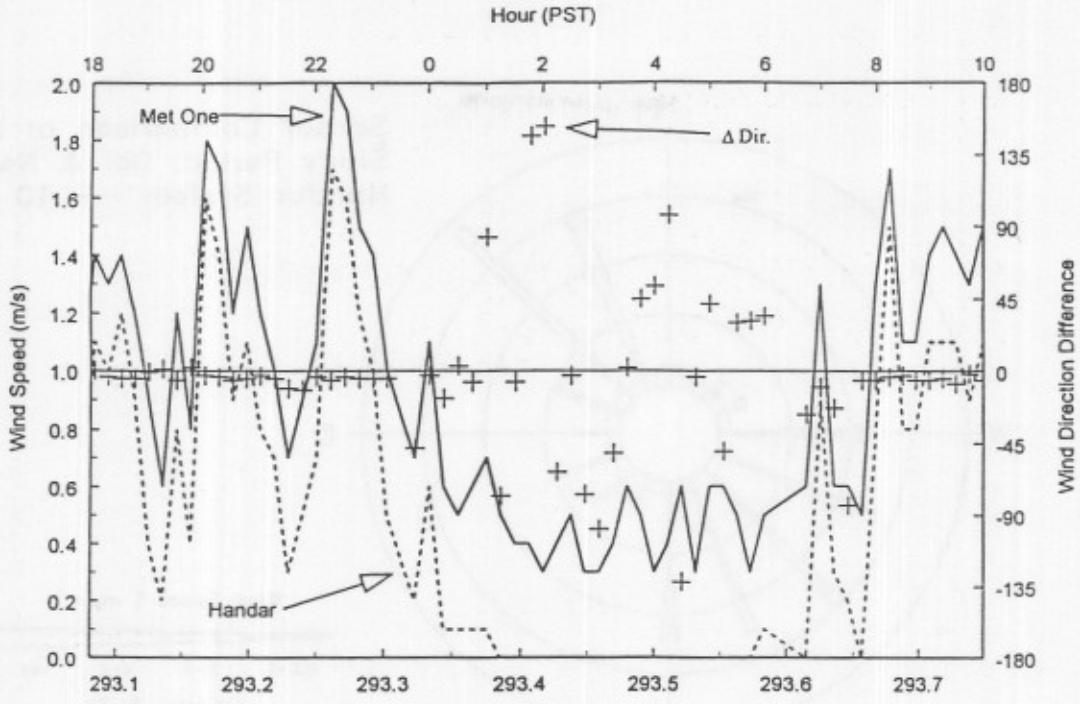

Figure 14. Time series of wind speeds at 10 m during a 16-hour period (19-20 Oct.) of winds <2 m/s.

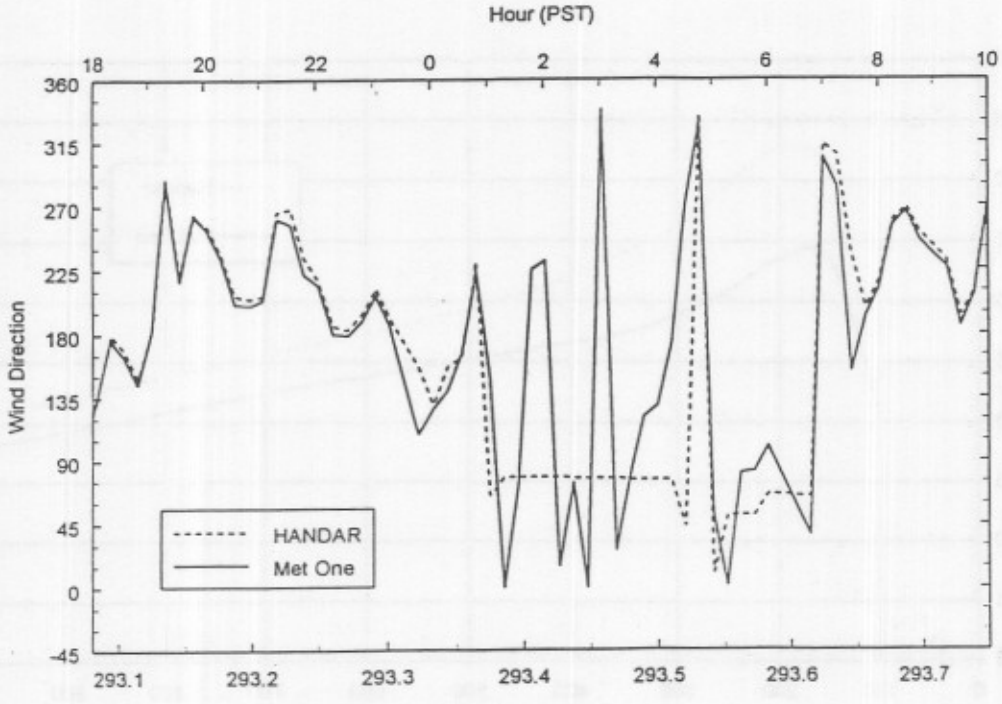

Figure 15. Wind direction for the Handar and Met One systems during the same period as Figure 14.

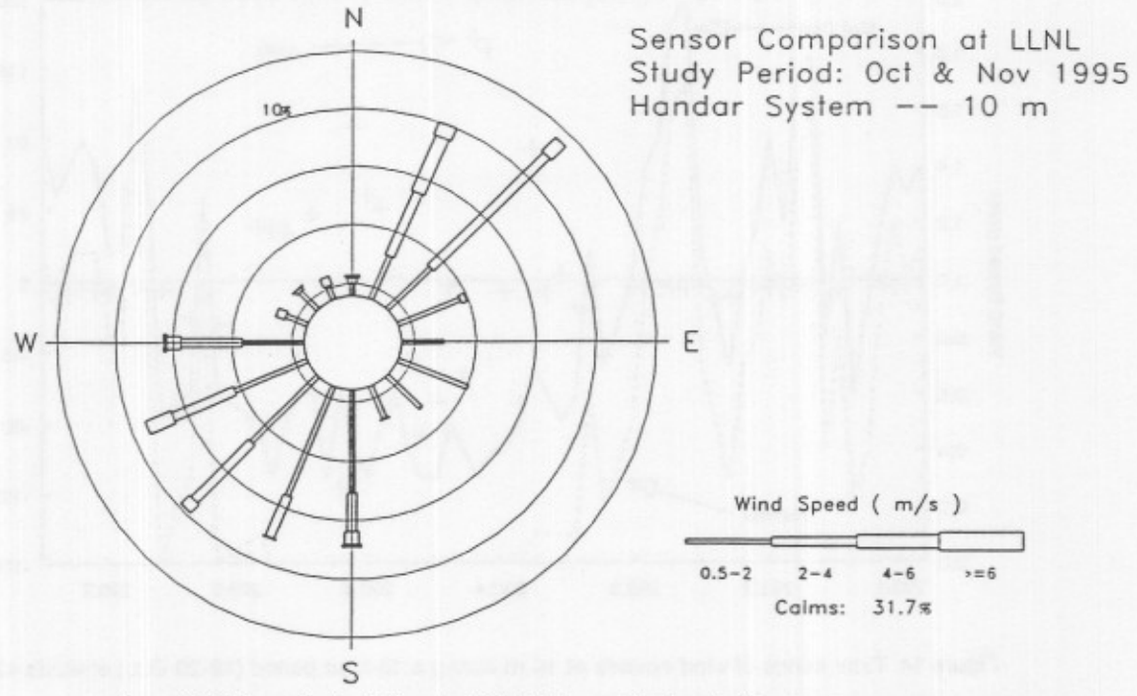

Figure 16. Wind rose for the study period. Wind data was taken from the Handar system at the 10-m level.

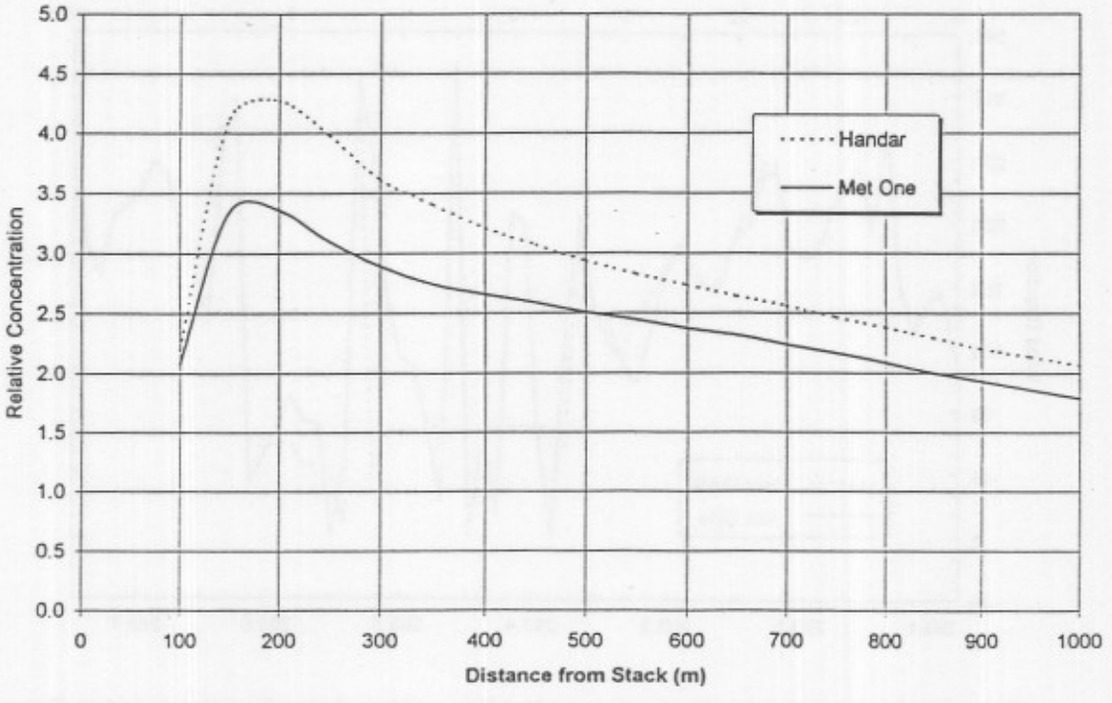

Figure 17. Average relative concentrations plotted against distance from the stack as modeled using CAP88-PC.